Type VII Collagen Is a Major Structural Component of Anchoring Fibrils

Lynn Y. Sakai,*‡ Douglas R. Keene,* Nicholas P. Morris,*‡ and Robert E. Burgeson*‡

*The Shriners Hospital for Crippled Children, and the ‡Department of Biochemistry, Oregon Health Sciences University, Portland, Oregon 97201

Abstract. Anchoring fibrils are specialized fibrous structures found in the subbasal lamina underlying epithelia of several external tissues. Based upon their sensitivity to collagenase and the similarity in banding pattern to artificially created segment-long spacing crystallites (SLS) of collagens, several authors have suggested that anchoring fibrils are lateral aggregates of collagenous macromolecules. We recently reported the similarity in length and banding pattern of anchoring fibrils to type VII collagen SLS crystallites. We now report the construction and characterization of a murine monoclonal antibody specific for type VII collagen. The epitope identified by this antibody has been mapped to the carboxyl terminus of the major helical domain of this molecule. The presence of type VII collagen as detected by indirect immunofluorescence in a variety of tissues corresponds exactly with ultrastructural observations of anchoring fibrils. Ultrastructural immunolocalization of type VII collagen using a 5-nm colloidal gold-conjugated second antibody demonstrates metal deposition upon anchoring fibrils at both ends of these structures, as predicted by the location of the epitope on type VII collagen. Type VII collagen is synthesized by primary cultures of amniotic epithelial cells. It is also produced by KB cells (an epidermoid carcinoma cell line) and WISH (a transformed amniotic cell line).

Downloaded from http://rupress.org/jcb/article-pdf/103/4/1577/1464785/1577.pdf by guest on 25 April 2024

ANCHORING fibrils are specialized fibrous structures (5, 29) found within the subbasal lamina in human and rat oral mucosa, amphibian skin and notocord, human and rat gingiva, human cervical mucosa, mouse uterus, and human vaginal mucosa, and also along Schwann cells in unmylelinated nerve fibers in human skin (21). Ultrastructurally, they have a centrosymmetric banding pattern suggesting that they are composed of an aligned lateral aggregate of individual anti-parallel fibrous subunits. The absolute length of these structures is difficult to determine because they undulate in and out of the plane of section, but the longest anchoring fibrils thus far documented approximate 750 nm in length (5). The presumed function of the anchoring fibril is to secure the lamina densa to the underlying connective tissue matrix by physical entrapment of major collagen fibers between the lamina densa and the anchoring fibril. The chemical nature of anchoring fibrils is unknown. Similarity of banding pattern of observed anchoring fibrils with that of artificially aggregated segment-long spacing crystallites (SLS crystallites)[1] of collagens (32) and their sensitivity to destruction by bacterial collagenase (19) suggest that aggregates of collagen may be the major structural component of the anchoring fibril. This concept was further strengthened by the observation that both the dimensions and the banding pattern of anchoring fibrils strongly resemble dimeric type VII collagen SLS crystallites (8). In this report, we confirm the identification of type VII collagen within the anchoring fibrils.

The importance of anchoring fibrils to the structural stability of skin is strongly supported by the observation that patients lacking anchoring fibrils, as determined by ultrastructural visualization, demonstrate the phenotype of epidermolysis bullosa dystrophica-recessive (3). These patients suffer extensive cutaneous blistering resulting from a separation of the dermis from the epidermis along the subbasal lamina.

Type VII collagen has recently been described (2, 28). After solubilization from amnion by limited proteolysis using pepsin, the type VII molecule is visualized by transmission electron microscopy after rotary shadowing as a 780-nm dimer of two identical molecules, each 424 nm in length associated through a 60-nm overlap of the triple-helical domains stabilized by disulfide bonds (28). Re-exposure of this molecule to pepsin under nondenaturing conditions cleaves each dimer into three components: two fragments denoted as P2, each 174 nm in length (which represent the carboxyl-terminal portions of the molecules), and a third peptide denoted as $(P1)_2$, 440 nm in length, which contains two 250-nm long peptides held together by disulfide bonds within a 60-nm overlap (see Fig. 9). Comparisons of the banding patterns of SLS crystallites made from type VII collagen dimers

1. *Abbreviations used in this paper*: ELISA, enzyme-linked immunosorbent assay; SLS crystallites, segment-long spacing crystallites.

© The Rockefeller University Press, 0021-9525/86/10/1577/10 $1.00

with anchoring fibrils indicate that the P2 peptides correspond to the region of anchoring fibrils at the site of insertion into the basal lamina and the $(P1)_2$ peptides correspond to the central region (8).

Materials and Methods

Preparation of Collagens

Type VII collagen and peptides P1 and P2 were prepared as previously described (2, 28). Collagen types I, III, and V were prepared from human amnion as detailed previously (6). Type II collagen was prepared from neonatal human femoral head cartilage as described (7). Collagen type IV was obtained from human placenta (33) and type VI was a generous gift from Dr. Robert Glanville (The Shriners Hospital for Crippled Children).

Monoclonal Antibody Production

A/J mice (Jackson Laboratories, Bar Harbor, ME) were immunized with 100 μg of human type VII collagen emulsified in complete Freund's adjuvant. 2 wk later mice were boosted on three consecutive days with 200 μg of human type VII collagen, and spleen cells were fused with the myeloma cell line P3-NS1/1-Ag4-1 (22) on the fourth day, according to previously described methods (18, 33). Hybridomas were screened for the production of antibody by the enzyme-linked immunosorbent assay (ELISA) and by indirect immunofluorescence, and selected colonies were cloned by limiting dilution.

Antibody was collected from selected hybridoma clones either in the form of spent tissue culture medium or as ascites from BALB/c x A/J hybrid mice, pristane primed, and injected with at least 10^7 hybridoma cells. For some experiments, ascites antibody was purified using DEAE Affi-gel Blue chromatography (Bio-Rad Laboratories, Richmond, CA), Protein A-Sepharose (Pharmacia Fine Chemicals, Piscataway, NJ), or type VII-coupled Sepharose.

ELISA

According to established methods (11), microtiter plates were coated with antigen (1–10 μg/ml) in bicarbonate-carbonate buffer, pH 9.6, overnight at 4°C, and were washed with phosphate-buffered saline (PBS)–0.05% Tween 20 to remove unadsorbed antigen. Hybridoma supernatants were diluted with PBS–0.05% Tween 20 and allowed to react with antigen-coated wells for 3 h at room temperature. After washing to remove unbound antibody, alkaline phosphatase–conjugated anti-mouse IgG (Sigma Chemical Co., St. Louis, MO) diluted in PBS–0.05% Tween 20 was incubated in the wells for 2 h, and after washing to remove unbound second antibody, substrate (*p*-nitrophenyl phosphate; Sigma Chemical Co.) was added. Absorbance was measured at 405 nm using Titertek Multiskan (Flow Laboratories, Inc., McLean, VA).

To screen hybridoma supernatants, type VII collagen was used to coat ELISA wells. In studies to determine cross-reactivity of the antibody with other collagens, types I–VII collagens were used as antigens.

To test the thermal stability of the antigenic site, type VII collagen was heated for 15 min at various temperatures, cooled rapidly in ice, and used to coat ELISA wells. Alternatively, 0.1 M 2-mercaptoethanol was added before heating to examine the effect of disulfide bonds on the stability of the antigenic site.

In experiments to determine the sensitivity of the antigenic site to Clostridial collagenase (Advance Biofactures, Lynbrook, NY), antigen-coated wells were incubated with collagenase in 50 mM Tris-HCl, pH 7.4, containing 10^{-3} M *N*-ethylmaleimide and 10^{-3} M $CaCl_2$ for 30 min at 30°C. After washing, the binding of antibody was tested as above.

Inhibition of antibody binding of type VII collagen was tested by incubating varying amounts of type VII collagen with a fixed amount of antibody and then incubating the mixture on type VII–coated ELISA wells.

Immunofluorescence

Tissues were frozen in liquid nitrogen, and 8-μm sections were cut using an American Optical histostat microtome at −28°C. Sections were air dried for 30 min and fixed in cold acetone for 10 min. After washing in PBS, sections were incubated with hybridoma supernatant for 2–3 h at room temperature, washed in PBS, and were then incubated with fluorescein-conjugated anti-mouse IgG (Sigma Chemical Co., St. Louis, MO) for 30 min. After washing, the sections were covered with 90% glycerol in PBS and were viewed using a Zeiss Photomicroscope III. Cell cultures (primary cultures of amniocytes and fibroblasts and established lines KB [10], WISH [15], HT1080 [12], and FL [30] from the American Type Culture Collection, Rockville, MD) grown on glass slides were fixed either in acetone or 2% paraformaldehyde, and were then tested as above.

Visualization of Antigen–Antibody Complexes

Purified antibody was incubated in approximately equimolar concentration with type VII collagen overnight at 4°C in 0.2 M NH_4HCO_3, pH 7.8. This mixture was then diluted with glycerol, sprayed, and rotary shadowed as previously described (9).

Immunoelectron Microscopy

En Bloc Labeling. Neonatal foreskin was obtained within 10 min after circumcision, and sliced into strips (which all included epithelium) ~0.5–1 mm in thickness with a double-edged razor blade. Tissue was then washed four times for 2 h at 4°C in 25 ml PBS, pH 7.4. The primary antibody was diluted 1:5 in PBS to 2 ml and incubated with the tissue at 4°C for 7–15 h. Samples were extensively rinsed in at least four changes of PBS at 4°C for a minimum of 7 h. The samples were then incubated with 5-nm gold conjugated to goat anti-mouse IgG (Jannsen Pharmaceuticals, Piscataway, NJ) diluted 1:2 in 1.0% BSA Buffer (20 mM Tris-HCl, 0.9% NaCl, 1 mg/ml BSA, 20 mM NaN_3), pH 8.0, for 5–15 h. The incubated samples were washed in PBS as above and then rinsed in 0.1 M sodium cacodylate buffer, pH 7.4, three times for 15 min. Rinsed samples were fixed in cacodylate-buffered Karnovsky's fix (20) for 60 min at 4°C, rinsed in buffer three times for 15 min per rinse at 4°C, and finally fixed in 1% OsO_4 in cacodylate for 60 min at 4°C. Fixed samples were rinsed in buffer three times for 15 min each time at 4°C, and dehydrated at room temperature through 30, 50, 70, 90, 95, and finally 100% ethanol. After two more changes of 100% ethanol over 30 min, samples were washed in 100% propylene oxide three times for 30 min each wash. Specimens were infiltrated with Spurr's epoxy (hard formula) embedded so as to obtain cross sections of epithelium and polymerized at 70°C overnight. 60–90-nm sections were cut on a Reichert Ultracut E Ultramicrotome and mounted on 2 × 1-mm formvar-coated slot grids. Grids were stained in 2% uranyl acetate in 50% ethanol for 15 min, and Reynold's lead citrate (31) for 60 s.

Section Surface Labeling of Lowicryl K4M–embedded Samples. Samples were fixed in 0.1 M phosphate-buffered picric acid/paraformaldehyde (35) on ice for 30 min. Samples were then rinsed in 0.1 M phosphate buffer over a 15-min period, then in 0.15 M Tris-HCl, pH 7.4, and again in phosphate buffer. Samples were then dehydrated on ice from 30 to 100% CH_3CH_2OH, then infiltrated in Lowicryl K4M (13), embedded in BEEM capsules so as to obtain cross sections of epithelium, and polymerized overnight at 4°C under ultraviolet (UV) light, then for an additional 2 d at ambient temperature. 90–110-nm thick ultrathin sections were cut and mounted on formvar-coated 2 × 1-mm Pd slot grids. Grids supporting sections were floated on two pools of twice-distilled H_2O over 10 min, for 15 min on a pool of 0.1% BSA buffer, pH 7.5, supplemented with 5% normal goat serum (total volume 300 μl) on a parafilm sheet for 120 min at ambient temperature. Grids were then washed quickly in BSA buffer, pH 7.5, twice in PBS, then again in BSA buffer. The grids were floated section-side down on 300-μl drops of 5-nm colloidal gold–conjugated goat anti-mouse IgG diluted 1:3 in 0.1% BSA buffer, pH 8.0, for 60 min at ambient temperature on parafilm in a covered petri dish, using moist filter paper to prevent evaporation. After incubation in gold complex, the grids were again floated on pools of BSA buffer and PBS as above, then on pools of twice-distilled water, and dried. Grids containing sections were then exposed to 0.1 M phosphate-buffered 1% OsO_4 vapors, stained in a 2% uranyl acetate in 50% CH_3CH_2OH for 15 min, and in Reynold's (31) lead citrate for 15 min before examination.

Specimens prepared by either technique were then examined at 60–80 kV using a 30-μm objective aperture with a Philips 410 L.S. transmission electron microscope. Magnification was calculated based on a carbon grating replica having 2,160 crossed lines per mm (Ernest F. Fullam, Inc., Schenectady, NY; cat No. 10021).

Results

Antibody Characterization

Hybridomas resulting from the fusion of spleen cells from type VII immunized mice with the myeloma line were cloned

Downloaded from http://rupress.org/jcb/article-pdf/103/4/1577/1464785/1577.pdf by guest on 25 April 2024

Table I. ELISA Reactivity

	A_{405} nm*	
	−collagenase	+collagenase
Anti-type VII (against type VII)	0.810 (100%)	0.180 (0%)
Anti-type VII (against P1 + P2)	0.15 (0%)	0.130 (0%)
Anti-type IV (against type IV)	0.790 (100%)	0.180 (0%)
Anti-type II (against type II)	0.625 (100%)	0.100 (0%)
Anti-NP32 (against crude NP)	0.390 (100%)	0.380 (95%)
Anti-NP161 (against crude NP)	0.375 (100%)	0.375 (100%)
PBS (against type VII)	0.180	0.181

* Values are averages of five independent determinations.

and screened for antigen binding by the ELISA. Immunopositive clones were then tested for the sensitivity of antibody binding to digestion of the substrate with clostridial collagenase. The reactivity of a monoclonal antibody to type IV (33) collagen before and after substrate collagenase digestion and the reactivity of a monoclonal antibody to type II (18) collagen before and after collagenase digestion of the substrate were used to demonstrate collagenase activity. The reactivity of two monoclonal antibodies (anti-NP32 and anti-NP161) (16) to noncollagen matrix proteins before and after collagenase digestion of the substrate were used to detect the activity of noncollagen-specific proteases in the collagenase preparations. The reactivity of the anti-type VII monoclonal antibody as well as the anti-type IV and anti-type II antibodies are completely susceptible to collagenase digestion of their respective substrates (Table I). Collagenase digestion of the substrate of anti-NP32 and anti-NP161 shows no significant diminution of reactivity. The results indicate that the anti-type VII collagen epitope resides within or very near a triple-helical sequence.

The ELISA reactivity of the anti-type VII monoclonal antibody can be fully inhibited by preincubation of the antibody with purified antigen. At a 1:8,000 dilution of ascites antibody, 2.5 μg of purified type VII collagen produces 100% inhibition as indicated in Fig 1.

Thermal stability of the epitope was tested by preincubating the antigen at 22, 40, 60, 80, and 100°C followed by rapid cooling and the ELISA (Fig. 2). Full activity is observed at 22 and 40°C with a gradual decrease in activity to background levels at 100°C. Inclusion of 2-mercaptoethanol in the incubation mixture causes a complete loss of reactivity above 40°C. An approximate 50% loss in activity is observed even at 22°C. No equivalent reduction in reactivity is seen for type III collagen in the presence or absence of 2-mercaptoethanol at 22°C using an anti-type III monoclonal antibody. These experiments indicate that disulfide bonds are involved in the stability of the type VII epitope. Once the disulfide bonds have been broken, reactivity is not regained above the denaturation temperature of the triple helix. These results suggest that the thermal stability of the epitope is dependent upon both an intact disulfide bond and the triple-helical conformation. Since interchain disulfide bonds have not been observed within the triple-helical structure, the

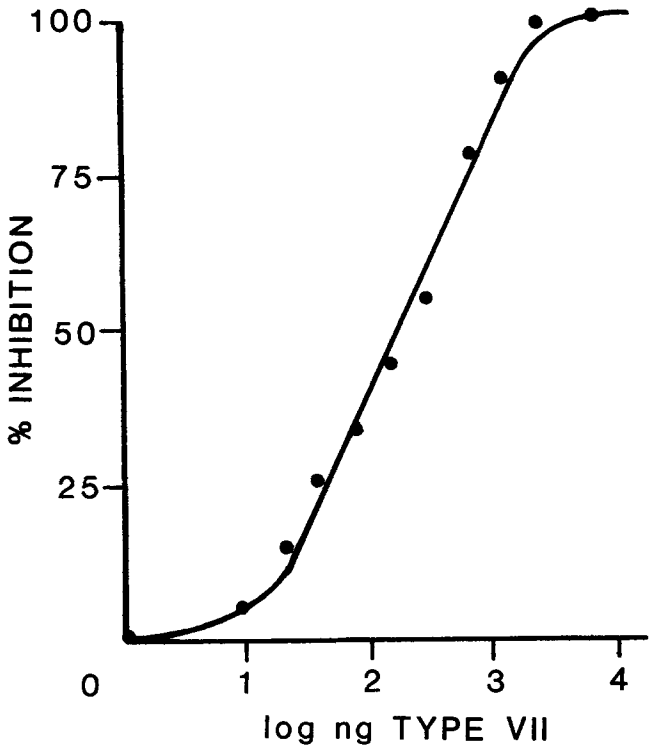

Figure 1. Competitive inhibition of monoclonal antibody binding to antigen with purified type VII collagen. Preincubation of the anti-type VII monoclonal antibody with type VII collagen at various concentrations inhibits antibody binding to antigen as measured by the ELISA. Maximal inhibition was observed at 2.5 μg. The antibody solution is a 1:8,000 dilution of ascites. Type VII collagen concentration was determined by amino acid analysis.

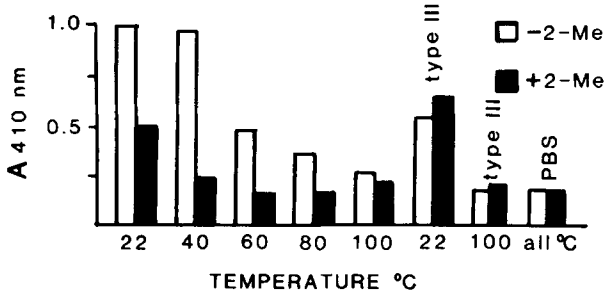

Figure 2. The effect of temperature and disulfide bond reduction upon the reactivity of the monoclonal antibody for type VII collagen. Antibody binding occurs at temperatures up to 40°C in the absence of 2-mercaptoethanol (*2-Me*) but is greatly reduced even at 22°C when the disulfide bonds of the substrate are dissociated. Binding of a type III-specific monoclonal antibody to type III collagen is unaffected by disulfide bond reduction but is sensitive to denaturation of the substrate. Conjugate binding in the absence of first antibody indicates background absorbance (*PBS*). All ELISAs were performed as described in Materials and Methods.

Downloaded from http://rupress.org/jcb/article-pdf/103/4/1577/1464785/1577.pdf by guest on 25 April 2024

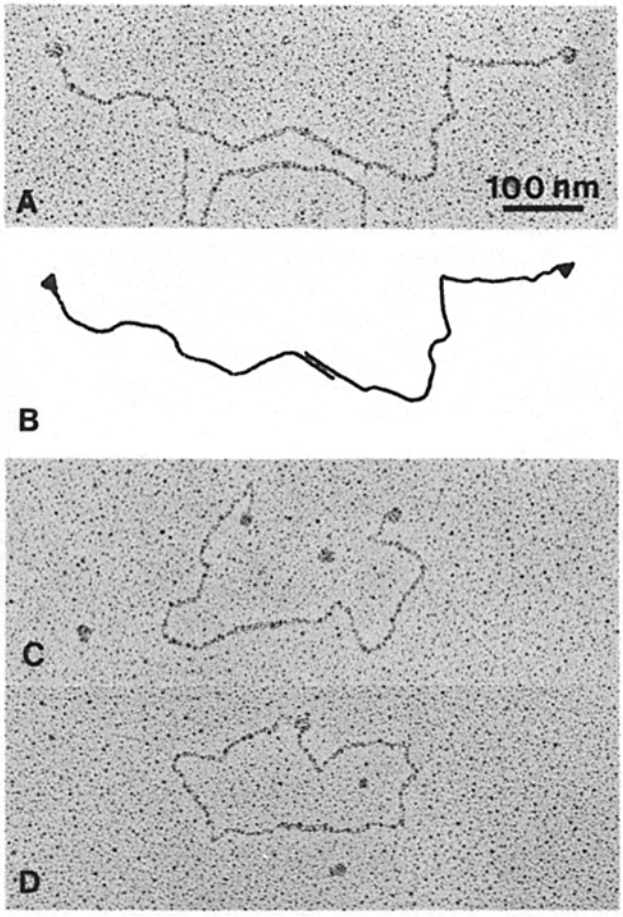

Figure 3. Transmission electron microscopical visualization of the monoclonal antibody–type VII collagen complex after rotary shadowing. The anti–type VII collagen monoclonal antibody is shown to bind the carboxyl-terminal ends of type VII dimers. Molecules with antibody at both termini are frequently seen (*A*, *C*; schematically represented in *B*). Bivalent binding of both ends by a single antibody is also observed (*D*).

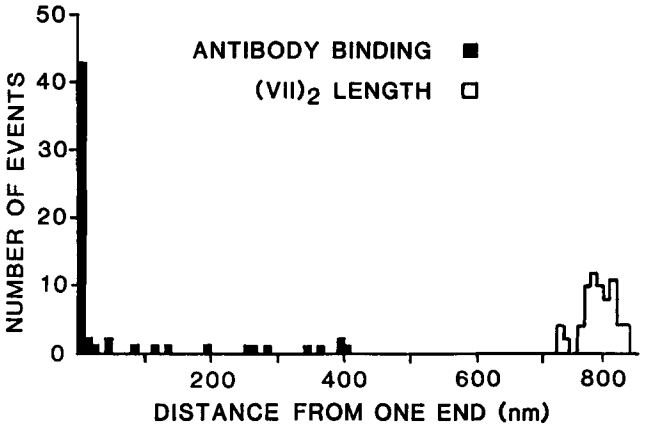

Figure 4. The relationship of the antibody binding site to molecular length. Antibody–antigen complexes were visualized after rotary shadowing and the positions of antibody molecules were measured relevant to the distance to the nearest molecular end (■). Only fully distended, non-overlapping dimeric molecules were measured. Any antibody touching an appropriate collagen molecule was scored. The total molecular lengths were also tallied (□). 60 molecules were measured. Greater than 70% of the observed binding events occurred within 10 nm of the carboxyl termini.

results suggest that the epitope is near the boundary between a triple-helical and a globular domain.

Redigestion of type VII collagen with pepsin under native conditions converts the type VII dimer to a dimer of P1 peptides and to P2 (2). Both the P1 dimer and P2 are independently disulfide bonded (28). Neither of these peptides is immunoreactive by the ELISA (Table I). Proteolytic activity of pepsin occurs at a triple-helical disruption between the P1 and P2 portions of the molecule and may also occur within non-triple-helical regions at the amino and/or carboxyl termini. Therefore, the data indicate that the epitope resides either within a non-triple-helical region at either end of the molecule or at the internal pepsin site.

The position of the epitope was demonstrated by visualizing the antibody–antigen complex by transmission electron microscopy after rotary shadowing. As shown in Figs. 3 and 4, antibody binds specifically to the carboxyl termini of the type VII dimer.

Antibody Specificity

The reactivity of the anti–type VII collagen antibody was tested versus human collagen types I–VII by ELISA (Table II). No reactivity above background levels was detected for any collagen type other than VII. The specificity of the antibody was further demonstrated by indirect immunofluorescence. Crisp, brilliant fluorescence is observed only at the basement membrane zone of the amniotic epithelial basement membrane and the zone underlying the basement membrane of the dermal–epidermal junction of skin (Fig. 5). No staining of the type IV–containing basement membranes surrounding the vasculature and adnexal structures of skin nor the trophoblastic membranes of chorioamnion is observed. Likewise, neither placenta nor muscle are stained. Additional staining of these tissues and of elastic cartilage is not revealed by pretreatment of the tissue with acetic acid (25), pepsin (37), or hyaluronidase (18) (data not shown). These observations indicate that the antibody recognizes an epitope specific to certain basement membrane zones. No staining is observed for any cartilagenous structures or for regions that contain types V or VI collagens. These data indicate that the antibody does not recognize any known collagen other than type VII.

Table II. Cross-reactivity of the Anti–type VII Collagen Monoclonal Antibody with Other Collagen Types Determined by ELISA

A_{405} nm*

Collagen type	Hybridoma culture media	Purified and diluted ascites	Culture media alone
I	0.021	0.015	0.011
II	0.019	0.015	0.013
III	0.022	0.005	0.007
IV	0.010	0.023	0.015
V	0.033	0.012	0.004
VI	0.025	0.011	0.004
VII	0.444	0.477	0.034

* Values are averages of three independent determinations.

Downloaded from http://rupress.org/jcb/article-pdf/103/4/1577/1464785/1577.pdf by guest on 25 April 2024

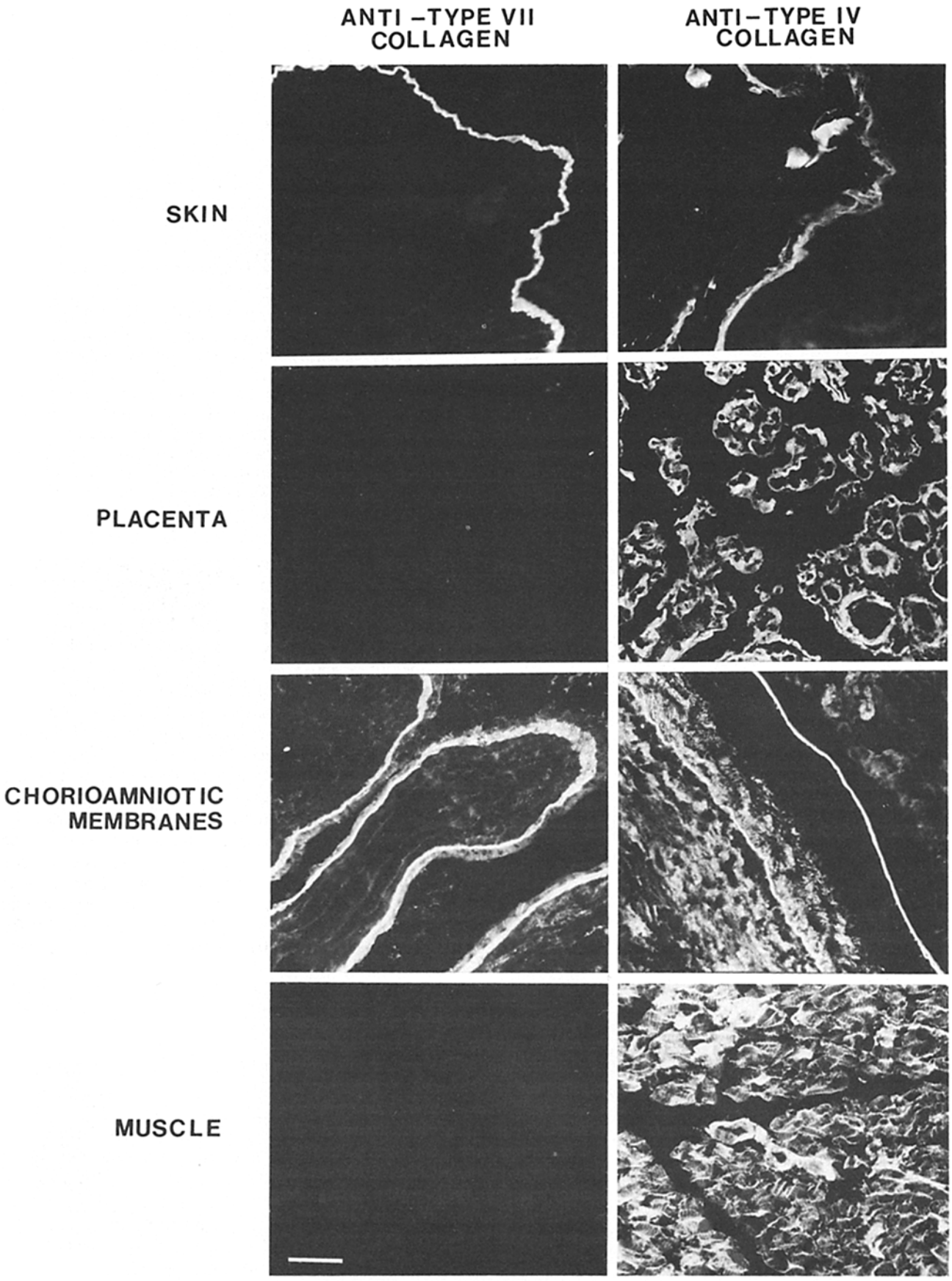

Figure 5. A comparison of indirect immunofluorescent patterns produced by monoclonal antibodies to type VII and type IV collagens. Monoclonal antibodies to type VII collagen specifically direct staining of the dermal–epidermal junction basement membrane zone of skin and the amniotic epithelial basement membrane of chorioamnion. The location of all basement membrane is indicated by the fluorescence directed by a monoclonal antibody to Type IV collagen (12). Bar, 50 μm.

Downloaded from http://rupress.org/jcb/article-pdf/103/4/1577/1464785/1577.pdf by guest on 25 April 2024

Table III. Correlation of the Presence of Type VII Collagen as Detected by Immunofluorescence with Anchoring Fibrils Detected Ultrastructurally

	Immunofluorescence	Anchoring fibrils (reference)
Skin	+	+(4)
Chorioamnion	+	+(8)
Placenta	−	−
Skeletal muscle	−	−
Cornea (Bowman's membrane)	+	+(27)
Oral mucosa	+	+(36)
Cervix	+	+(23)
Kidney cortex	−	−
Lung alveoli	−	−
Liver sinusoids	−	−
Stomach (fundus)	−	−
Large intestine	−	−
Elastic cartilage	−	−

Tissue Distribution of Antigen

The presence of antigen in foreskin, chorioamnion, placenta, skeletal muscle, cornea, oral mucosa, cervix, kidney cortex, lung, liver, stomach, large intestine, and elastic cartilage was separately tested by indirect immunofluorescence. As indicated in Table III, fluorescent staining was observed only along the dermal-epidermal basement membrane zone of skin, the amniotic epithelial basement membrane zone of chorioamnion, the epithelial basement membrane of oral mucosa and cervix, and corneal epithelial basement membrane but not Descemet's membrane. Kidney, lung, liver, stomach, intestine, and elastic cartilage were unstained. Results demonstrate that there is a direct correlation of antibody-directed fluorescent staining and the ultrastructural observation of anchoring fibrils.

The ability of various cell types to synthesize type VII collagen was also analyzed by indirect immunofluorescence. Primary cultures of amniotic epithelial cells demonstrate strong fluorescent staining. The oral epidermal carcinoma cell line KB (10) and the transformed epithelial cell line WISH (15) also show equal intracellular stain intensity (Fig. 6). Primary cultures of dermal fibroblasts are sometimes stained. Cell lines HT 1080 (12), a human fibrosarcoma which secretes basement membrane components (1), and FL (30), a transformed amniotic epithelial cell, showed no fluorescence when identically treated (not shown).

Ultrastructural Immunolocalization of Type VII Collagen

Ultrastructural immunolocalization of type VII collagen in human skin was performed as described in Materials and Methods. Using a colloidal gold-conjugated second antibody, metal deposition is detected only in the subbasal lamina of the dermal-epidermal junction (Fig. 7). The gold is concentrated within 1.5 μm of the lamina densa with nearly no gold deposited anywhere else within the dermis or the basal cell layer. Deeper regions of the dermis are accessible to antibody under the conditions used as shown by deposition of gold between matrix microfibrils directed by an anti-microfibril monoclonal antibody (34) (Fig. 8 *A*). In addition, this antibody directed no labeling of anchoring fibrils but rather is specific for microfibrils, even though it is of the same immunological subtype as the anti-type VII antibody.

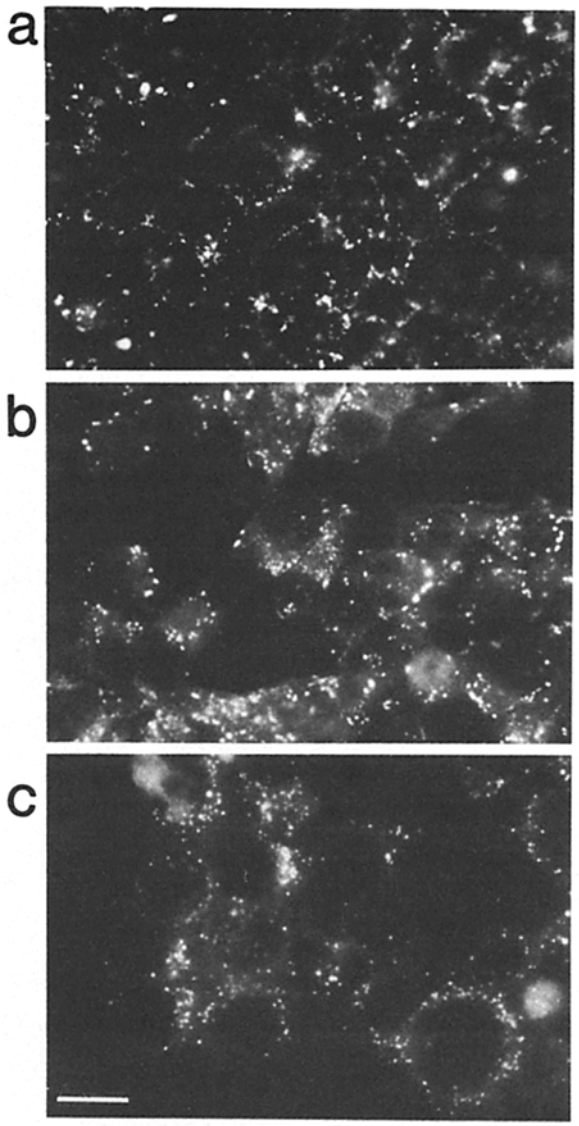

Figure 6. Indirect immunofluorescent staining of cultured cells by the anti-type VII collagen antibody. Indirect immunofluorescence of KB (*c*) and WISH (*b*) cells in culture, fixed in acetone and displaying intracellular staining of type VII collagen. WISH cells, fixed in 2% paraformaldehyde (*a*), show extracellular matrix deposition of type VII collagen. Bar, 50 μm.

Figure 7. Ultrastructural immunolocalization of anti-type VII collagen monoclonal antibody to anchoring fibrils. A monoclonal antibody specifically recognizing the terminal ends of type VII collagen dimers directs the deposition of colloidal gold to the ends of the anchoring fibrils. Abundant gold deposition was apparent upon the dermal ends of anchoring fibrils (*C* and *F–K*). Less gold was deposited along the lamina densa due to restricted access of the antibody to that region which is characteristic of the en bloc technique. Gold deposits are frequently seen in regions where anchoring fibrils intersect "amorphous patches" in the dermis (*A*, *B*, and *D*). Banded collagen fibers are often seen entrapped within the anchoring fibril arches (*A*, *E*, *I*, and *J*). *B–K* are higher magnification images than *A*. Bars, 250 nm.

Downloaded from http://rupress.org/jcb/article-pdf/103/4/1577/1464785/1577.pdf by guest on 25 April 2024

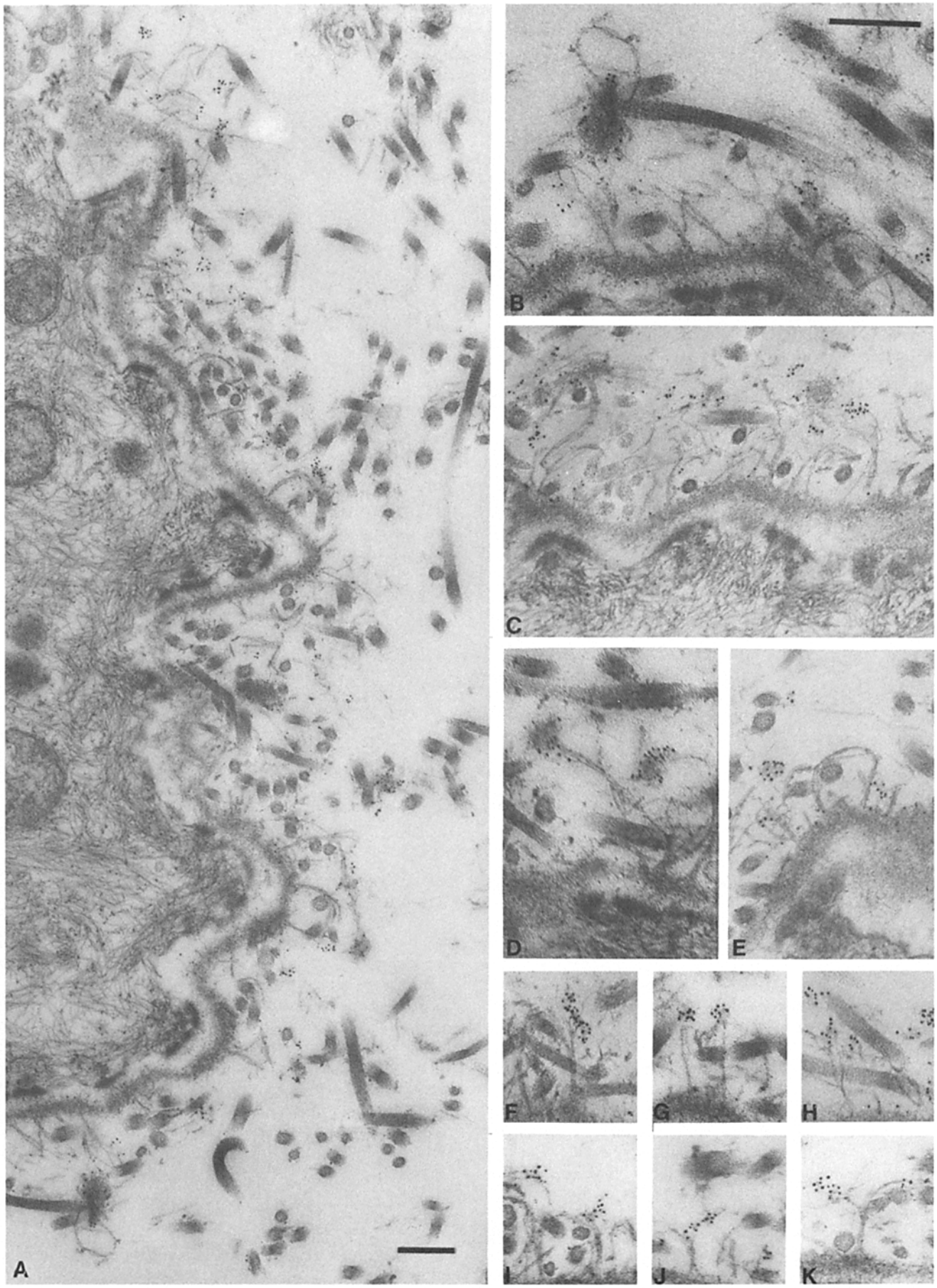

Downloaded from http://rupress.org/jcb/article-pdf/103/4/1577/1464785/1577.pdf by guest on 25 April 2024

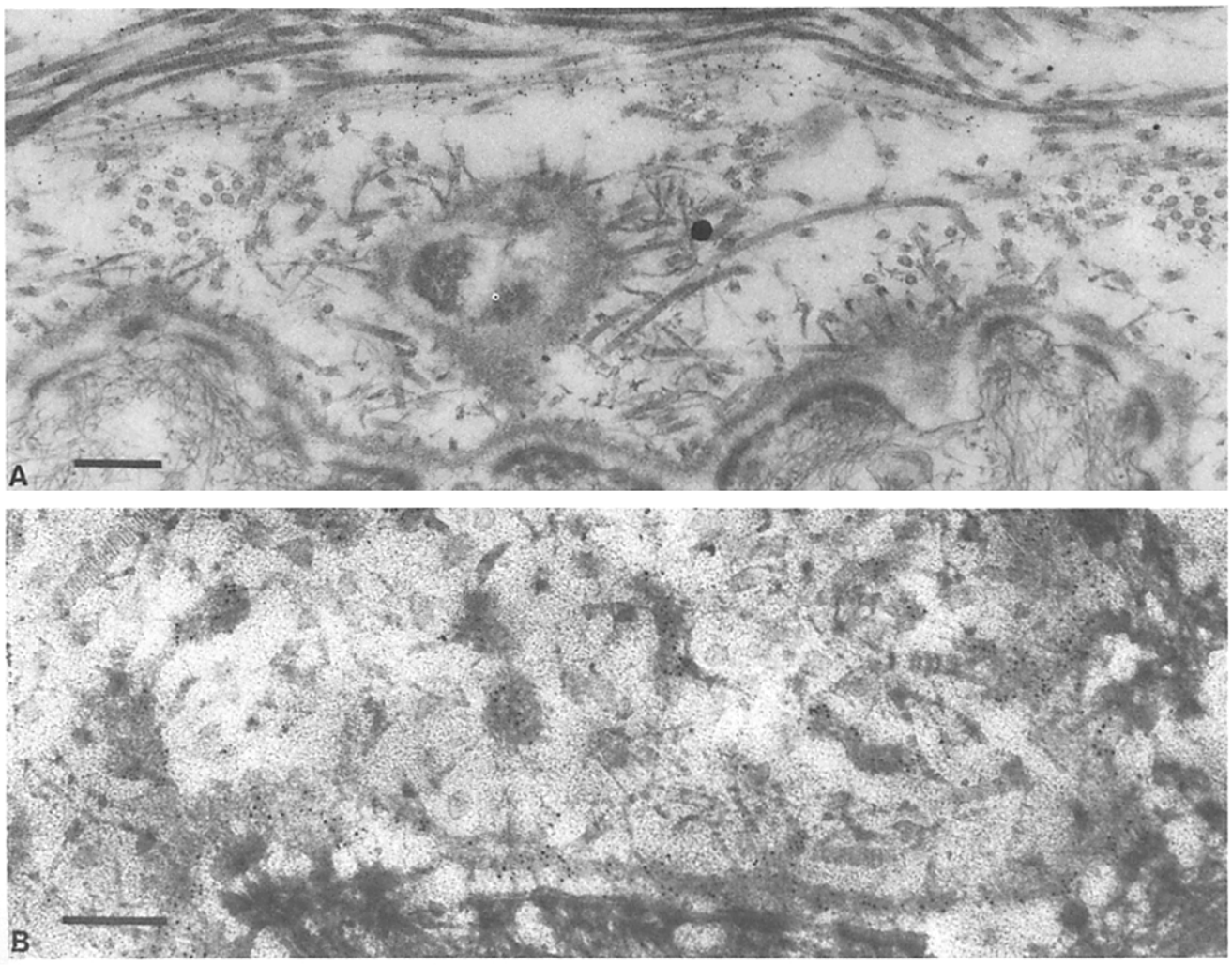

Figure 8. Ultrastructural localization of microfibrillar antigen by the en bloc method and type VII collagen by surface labeling. (*A*) A monoclonal antibody (IgG) to microfibrillar antigen (34) directed 5-nm colloidal gold to microfibrils near the dermal–epidermal junction of foreskin, but did not direct label to anchoring fibrils nor to terminal dermal patches. Bar, 250 nm. (*B*) Anti-type VII directed gold label to the entire lamina densa as well as the subbasal lamina when applied to the section surface of Lowicryl K4M-embedded skin, followed by 5-nm colloidal gold-conjugated second antibody. Bar, 250 nm.

No metal deposition was detected in control experiments lacking first antibody (not shown).

Surface labeling of a thin section taken from Lowacryl K4M-embedded neonatal foreskin using the anti-type VII collagen antibody is shown in Fig. 8 *B*. With this methodology, gold deposition is observed along the entire lamina densa of the dermal–epidermal basement membrane in addition to regions of the subbasal lamina. Again, no labeling was observed in the absence of first antibody (not shown). Control experiments using antibodies of the same immunological subtype, but with specificities not relevant to basement membrane components, show no gold deposition upon the basement membrane, nor within the subbasal lamina (not shown). These results clearly show the presence of antigen both within the lamina densa and the subbasal lamina. Surface labeling has the disadvantage that distinct anchoring fibrils are difficult to visualize.

Together, the en bloc and surface labeling procedures demonstrated specific gold labeling of both ends of anchoring fibrils as predicted by the known location of the epitope within type VII collagen and the proposed relationship of type VII collagen to anchoring fibrils.

Gold depositions frequently occurred upon the dermal terminii of anchoring fibrils as predicted by the known terminal location of the epitope in type VII collagen. These dermal termini often were seen inserting into an amorphous feltwork as previously described (27). These amorphous patches label intensely with the antibody. The sites of labeling of these patches coincide with locations of anchoring fibril insertion. These studies demonstrate that type VII collagen is located in the subbasal lamina of the dermal–epidermal junction of skin. The data further demonstrate that the carboxyl terminii of anchoring fibrils insert into the lamina densa and extend into the dermis as well, often ending in an amorphous feltwork.

Discussion

The observation of antibody-directed gold deposition upon ultrastructurally identified anchoring fibrils using a well-

Downloaded from http://rupress.org/jcb/article-pdf/103/4/1577/1464785/1577.pdf by guest on 25 April 2024

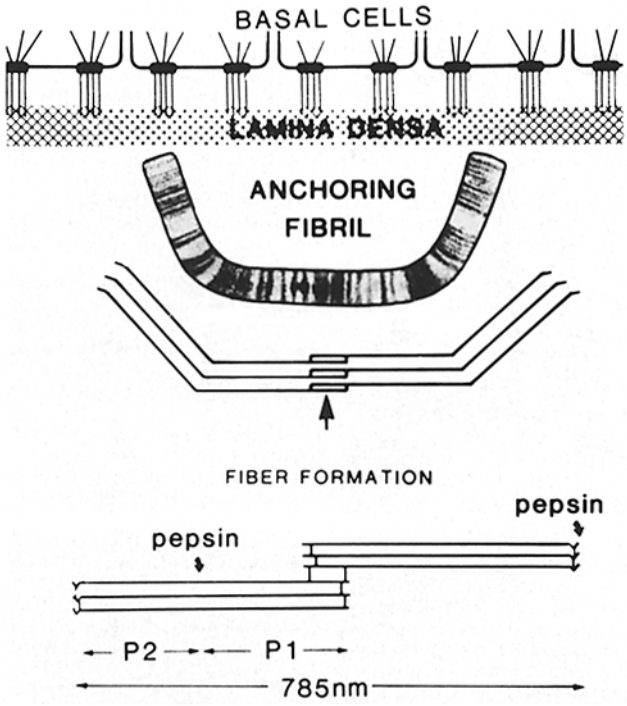

Figure 9. The proposed relationship of type VII collagen to anchoring fibrils. The illustration depicts the known structure of type VII collagen (9). In the lower portion of the figure, the three α chains of each dimeric type VII collagen molecule are shown. Interconnecting lines indicate the sites of disulfide bonds. Dimerization occurs at the amino-terminal ends of the molecules (9). Fiber formation is proposed to occur by unstaggered lateral association of type VII collagen dimers (middle portion of the figure). This aggregate is proposed to correspond to the banded anchoring fibril. The interaction of type VII collagen (and the anchoring fibril) with the lamina densa is believed to be mediated by a non-triple helical portion of type VII collagen lost during proteolytic solubilization. The model is consistent with the observed lengths of anchoring fibrils and type VII collagen dimers, with the similarity of banding patterns of type VII collagen SLS crystallites and ultrastructurally visualized anchoring fibrils, with the tissue distribution of type VII collagen and anchoring fibrils, and with the deposition of colloidal gold upon anchoring fibrils directed by a type VII-specific monoclonal antibody.

characterized monoclonal antibody, together with the correlation of dimensions and banding patterns of type VII collagen SLS crystallites with those of anchoring fibrils (8), in addition to the exact correlation of tissue distribution and location between type VII collagen and anchoring fibrils, allow us to conclude that type VII collagen is a major structural component of anchoring fibrils.

Anti-type VII collagen-directed gold deposition within the subbasal lamina of skin is very often seen over electron-dense amorphous patches (see Fig. 7). While these structures have been thought to be undulations of basement membranes, we and others (27) have observed these materials at locations quite distant from the lamina densa.

The identification of anchoring fibrils as the tissue form of type VII collagen suggests that the fiber form of the molecule is an unstaggered parallel array of dimeric type VII molecules. The anchoring fibril is the first observed collagenous structure which uses this aggregation method in vivo. Fig. 9 depicts the proposed relationship of type VII collagen dimers to the structure of anchoring fibrils. Attempts to form these structures in vitro under physiological conditions have thus far failed. The fiber-forming mechanism for type VII collagen is likely to involve non-helical domains at the carboxyl termini which are lost during pepsin solubilization of the tissue (26).

The observation of intracellular indirect immunofluorescence of normal and malignant epithelial cells directed by type VII-specific antibodies suggests that anchoring fibrils are products of the epithelium. Staining of dermal fibroblast cultures is occasionally seen, but it is our impression from biosynthetic studies of epithelial cells (26) and fibroblasts the amount of type VII made by fibroblasts is relatively minor. However, these cells can make detectable amounts of both types IV and VII collagens (Sakai, L., unpublished observations). The extent to which fibroblast products contribute to the structure of the lamina densa or to anchoring fibrils is unknown.

Monoclonal antibodies AF1 and AF2 have been previously reported to stain anchoring fibrils (14). However, these antibodies do not direct staining of fetal human skin before 26 wk of gestation (24) even though anchoring fibrils can be visualized ultrastructurally by 10 wk (17). The antibody we have described here specifically stains the fetal dermal-epidermal junction as early as week 7 of gestation, as one would expect for a major anchoring fibril component (Smith, L., unpublished observations). These results suggest that either additional components become associated with anchoring fibrils later in development, or AF1 and AF2 may recognize cross-link sites in type VII collagen or specific conformations dependent upon a state of aggregation which occurs subsequent to anchoring fibril synthesis and secretion.

The authors wish to recognize the significant contribution of Dr. Romaine Bruns, Harvard University, Massachusetts General Hospital, for his recognition of the similarity of type VII collagen and anchoring fibrils, and the gift of type VI collagen from Dr. Robert Glanville. The authors further gratefully acknowledge the technical contributions of Susan Holveck, Eileen Roux, and Marie Spurgin to this project.

These studies were supported by the Shriners Hospital for Crippled Children, grants AM35532 and AM33946 from the United States Public Health Service to R. E. Burgeson, the R. Blaine Bramble Medical Research Foundation, and the Fred Meyer Charitable Trust.

Received for publication 7 January 1986, and in revised form 15 April 1986.

References

1. Alitalo, K., A. Vaheri, T. Krieg, and R. Timpl. 1980. Biosynthesis of two subunits of type IV procollagen and of other basement membrane proteins by a human cell line. *Eur. J. Biochem.* 109:247-255.

2. Bentz, H., N. P. Morris, L. W. Murray, L. Y. Sakai, D. W. Hollister, R. E. Burgeson. 1983. Isolation and partial characterization of a new human collagen with an extended triple-helical structural domain. *Proc. Natl. Acad. Sci. USA.* 80:3168-3172.

3. Briggaman, R. A., C. E. Wheeler, Jr. 1975. Epidermolysis bullosa dystrophica-recessive: a possible role of anchoring fibrils in the pathogenesis. *J. Invest. Dermatol.* 65:203-211.

4. Brody, I. 1960. The ultrastructure of the tonofilaments in the keratinization process of normal human epidermis. *J. Ultrastruct. Res.* 4:264-297.

5. Bruns, R. R. 1969. A symmetrical extracellular fibril. *J. Cell Biol.* 42:418-430.

6. Burgeson, R. E., F. A. El Adli, I. I. Kaitila, and D. W. Hollister. 1976. Fetal membrane collagens: identification of two new collagen alpha chains. *Proc. Natl. Acad. Sci. USA.* 73:2579-2583.

7. Burgeson, R. E., P. A. Hebda, N. P. Morris, and D. W. Hollister. 1982. Human cartilage collagens. Comparison of cartilage collagens with human type V collagen. *J. Biol. Chem.* 257:7882-7886.

8. Burgeson, R. E., N. P. Morris, L. W. Murray, K. G. Duncan, D. R. Keene, and L. Y. Sakai. 1986. The structure of type VII collagen. *Ann. NY Acad. Sci.* In press.

Downloaded from http://rupress.org/jcb/article-pdf/103/4/1577/1464785/1577.pdf by guest on 25 April 2024

9. Dieringer, H., D. W. Hollister, R. W. Glanville, L. Y. Sakai, and K. Kuhn. 1985. Structural studies of human basement membrane collagen with the use of a monoclonal antibody. *Biochem. J.* 227:217–222.

10. Eagle, H. 1955. Propagation in fluid medium of human epidermoid carcinoma, strain K13. *Proc. Soc. Exp. Biol. Med.* 89:362–364.

11. Engvall, E., and P. Perlmann. 1972. Enzyme-linked immunosorbent assay, ELISA. *J. Immunol.* 109:129–135.

12. Fogh, J., and R. Lund. 1957. Continuous cultivation of epithelial cell strain (FL) from human amniotic membrane. *Proc. Soc. Exp. Med.* 94:532.

13. Garavito, R. M., W. Villager, and E. Carlemalm. 1980. Advances in specimen preparation for electron microscopy. I. Novel low-temperature embedding resins and a reformulated Vestopal. *Abstracts Experimentia.* 36: 740.

14. Goldsmith, L. A., and R. A. Briggaman. 1983. Monoclonal antibodies to anchoring fibrils for the diagnosis of epidermolysis bullosa. *J. Invest. Dermatol.* 81:464–466.

15. Hayflick, L. 1961. Propagation in fluid medium of human epidermoid carcinoma, strain KB. *Proc. Soc. Exp. Biol. Med.* 89:362–364.

16. Hessle, H., L. Y. Sakai, D. W. Hollister, R. E. Burgeson, and E. Engvall. 1984. Basement membrane diversity detected by monoclonal antibodies. *Differentiation.* 26:49–54.

17. Holbrook, K. A., and L. T. Smith. 1981. Ultrastructural aspects of human skin during embryonic, fetal, premature, neonatal, and adult periods of life. *Birth Defects.* 17:9–38.

18. Hollister, D. W., L. Y. Sakai, N. P. Morris, L. H. Shimono, and R. E. Burgeson. 1982. Production and characterization of a hybridoma antibody to native human type II collagen. *Collagen Relat. Res.* 2:197–210.

19. Kahl, F., and R. Pearson. 1967. Ultrastructural studies of experimental vesiculation. II. Collagenase. *J. Invest. Dermatol.* 49:616–631.

20. Karnovsky, M. J. 1965. A formaldehyde-gluteraldehyde fixative of high osmolality for use in electron microscopy. *J. Cell Biol.* 27(2, Pt.2):137*a*.

21. Kawanami, O., V. J. Ferrans, W. C. Roberts, R. G. Crystal, and J. D. Fulmer. 1978. Anchoring fibrils. A new connective tissue structure in fibrotic lung disease. *Am. J. Pathol.* 92:389–403.

22. Kohler, G., S. C. Howe, and C. Milstein. 1976. Fusion between immunoglobin-secreting and nonsecreting myeloma cell lines. *Eur. J. Immunol.* 6:292–295.

23. Laguens, R. 1972. Subepithelial fibrils associated with the basement membrane of human cervical epithelium. *J. Ultrastruct. Res.* 41:202–208.

24. Lane, A. T., K. F. Helm, and L. A. Goldsmith. 1985. Identification of bullus pemphigoid, pemphigus, laminin, and anchoring fibril antigens in human fetal skin. *J. Invest. Dermatol.* 84:27–30.

25. Linsenmayer, T. F., J. M. Fitch, T. M. Schmid, N. B. Zaic, E. Gibney, R. D. Sanderson, and R. Mayne. 1983. Monoclonal antibodies against chicken type V collagen: production, specificity, and use for immunocytochemical localization in embryonic cornea and other organs. *J. Cell Biol.* 96:124–132.

26. Lunstrum, G. P., L. Y. Sakai, D. R. Keene, N. P. Morris, and R. E. Burgeson. 1986. Large complex globular domains of type VII procollagen contribute to the structure of anchoring fibrils. *J. Biol. Chem.* In press.

27. McTigue, J. W., and B. S. Fine. 1966. The basement membrane of the corneal epithelium. *In* Electron Microscopy, 6th International Congress, Vol. 2. R. Uyeda, editor. Tokyo Marugen Co. Ltd. 775.

28. Morris, N. P., D. R. Keene, R. W. Glanville, and R. E. Burgeson. 1986. The tissue form of type VII collagen is an antiparallel dimer. *J. Biol. Chem.* 261:5638–5644.

29. Palade, G. E., and M. G. Farquhar. 1965. A special fibril of the dermis. *J. Cell Biol.* 26:263–291.

30. Rasheed, S. 1974. Characterization of a newly derived human sarcoma cell line. *Cancer.* 33:1027–1033.

31. Reynolds, E. S. 1963. The use of lead citrate at high pH as an electron-opaque stain in electron microscopy. *J. Cell Biol.* 17:208–215.

32. Rowlatt, C. 1969. Subepithelial fibrils associated with the basal lamina under simple epithelia in mouse uterus: possible tropocollagen aggregate. *J. Ultrastruct. Res.* 26:44–51.

33. Sakai, L. Y., E. Engvall, D. W. Hollister, and R. E. Burgeson. 1982. Production and characterization of a monoclonal antibody to human type IV collagen. *Am. J. Pathol.* 108:310–318.

34. Sakai, L. Y., D. R. Keene, and E. Engvall. 1986. Fibrillin, a new 350-kD glycoprotein, a component of extracellular microfibrils. *J. Cell Biol.* In press.

35. Stefanini, M., C. DeMartino, and L. Zamboni. 1967. Fixation of ejaculated spermatozoa for electron microscopy. *Nature (Lond.).* 216:173–174.

36. Susi, F. R., W. D. Belt, and J. W. Kelly. 1967. Fine structure of fibrillar complexes associated with the basement membrane in human oral mucosa. *J. Cell Biol.* 34:686–690.

37. von der Mark, K., and M. Ocalan. 1982. Immunofluorescent localization of type V collagen in the chick embryo with monoclonal antibodies. *Collagen Relat. Res.* 2:541–555.

Downloaded from http://rupress.org/jcb/article-pdf/103/4/1577/1464785/1577.pdf by guest on 25 April 2024